CASE STUDY

Coherent Charge Oscillations in Graphene Quantum Dots

Using an AWG and microwave generator setup controlled by Labber

KEYSIGHT

Abstract

The coherent dynamics of a quantum mechanical two-level system can give rise to quantum interference phenomena and allows for quantum interference spectroscopy. Interference spectroscopy can be exploited to study charge noise and charge decoherence in semiconductor quantum dots (QDs). Bilayer graphene serves as a promising host material for highly tunable QDs with a potential application as spin and valley qubits. Only recently, coherent charge oscillations have been reported in a bilayer graphene double QD. In this system, T_2^* charge decoherence times have been measured independently using Landau-Zener-Stückelberg-Majorana (LZSM) interference and photon assisted tunneling, consistently yielding T_2^* -times in a range of 400 to 500 ps[1]. In this case study, we provide an introduction into the measurement of coherent charge oscillations using a Keysight arbitrary waveform generator (AWG) and an analog microwave source. All experiments are controlled using the lab control and automation software, Labber.

Quantum dots in bilayer graphene

The weak spin-orbit and hyperfine interaction together with a gate-voltage-controllable band gap makes bilayer graphene (BLG) an interesting host material for spin and valley qubits. Gate voltages are used to confine electrons in BLG quantum dots (see Figure 1a, b), control the electrochemical potential of the QDs and their mutual coupling. Recent achievements in this field include the understanding of the spin-valley coupling, measurements of spin and valley relaxation times and the demonstration of electron-hole blockade.

This case study focuses on the measurement of coherent charge oscillations in a BLG double QD. The charge degree of freedom offers fast dynamics that can be controlled all-electrically, which in turn poses high demands on the control electronics requiring pulse widths on a sub-nanosecond time scale. Figure 1c shows a charge stability diagram characteristic for a double QD in the few electron regime. Figure 1d labels the ground states $|L\rangle$ and $|R\rangle$ forming a two-level system corresponding to an excess electron being in either in the left or right QD, respectively.

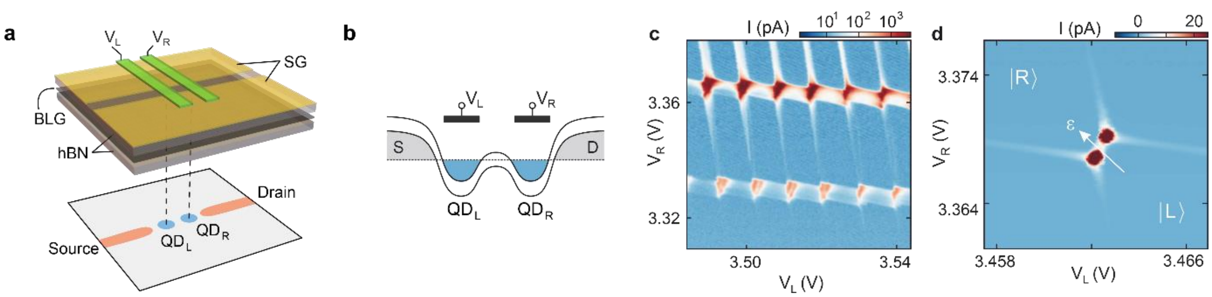

Figure 1. a Schematic cross-section of the device. Two layers of metallic gates are deposited on top of a heterostructure of bilayer graphene (BLG) and hexagonal boron nitride (hBN). Below, the charge carrier density is color coded indicating a p-type channel (red) and two electron QDs (blue). **b** Schematic band edge profile along the narrow channel. The voltages V_{L} and V_{R} applied to the finger gates form a double QD between the source and the drain reservoirs. **c** Charge stability diagram of the double QD at a low electron occupation (measured at a temperature of 20 mK). The current through the device is measured as a function of the gate voltages V_{L} and V_{R}. **d** Close-up of a pair of triple points highlighting the ground states $|L\rangle$ and $|R\rangle$.

Photon assisted tunnelling

Photon assisted tunneling (PAT) spectroscopy is an important tool to characterize the energy dispersion of a two-level system. Here, the two-level system is formed by the states $|L\rangle$ and $|R\rangle$ as depicted in Figure 1d. In order to drive resonant transitions between the ground and an excited state, a microwave signal is applied to one of the gates (see Figure 2a). Figure 2b shows the energy diagram of the two-level system as a function of the detuning ε. At finite tunnel coupling Δ, the states $|L\rangle$ and $|R\rangle$ hybridize, which is illustrated in the Bloch sphere representation (Figure 2c). PAT spectroscopy allows to map out the dispersion, and to determine the tunnel coupling from the resonance condition $hf = \sqrt{\varepsilon^2 + \Delta^2}$ (Figure 2d). Furthermore, PAT spectroscopy probes the coherent properties of the two-level system. From the full width at half maximum of the PAT resonances, the ensemble charge decoherence time T_2^* can be estimated.

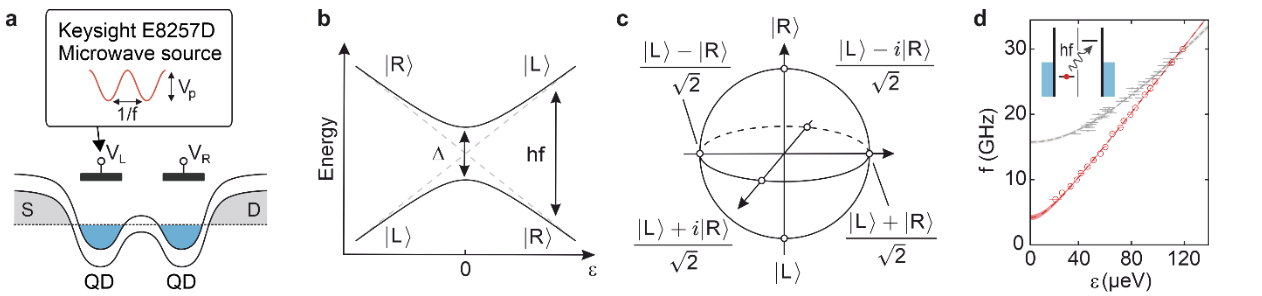

Figure 2. a Microwave excitation (frequency range $f = 0 - 30$ GHz) generated by a Keysight E8257D analog signal generator is applied to one of the finger gates controlling the double QD. **b** Energy diagram of the two-level-system. At finite tunnel coupling Δ, the states $|L\rangle$ and $|R\rangle$ hybridize, leading to a splitting of the eigenenergies of Δ at zero detuning. The resonance condition required for PAT is given by condition $hf = \sqrt{\varepsilon^2 + \Delta^2}$. **c** Bloch sphere representation of the two-level-system with the charge states $|L\rangle$ and $|R\rangle$ on the poles. **d** PAT spectroscopy showing the resonant excitation frequency f as a function of the detuning between the two QDs for two different tunnel couplings.

Landau-Zener-Stückelberg-Majorana interference spectroscopy

Landau-Zener-Stückelberg-Majorana (LZSM) interference spectroscopy is a powerful tool to probe the dynamics of a two-level system and to determine the charge decoherence time. For that purpose, the two-level system is driven non-adiabatically through the anti-crossing of the energy levels at $\varepsilon = 0$. Probing decoherence times in the sub-nanosecond regime poses strong requirements on the pulse generator and on the RF installation in the cyostat. A Keysight M8195A AWG with a sampling rate of 65 GS/s is used to generate pulse sequences with the shortest pulse width of 30 ps (Figure 3a). During the time span t_p the system picks up a phase (Figure 3b), which results in the observation of coherent oscillations in the time domain as shown exemplarily in Figure 3c.

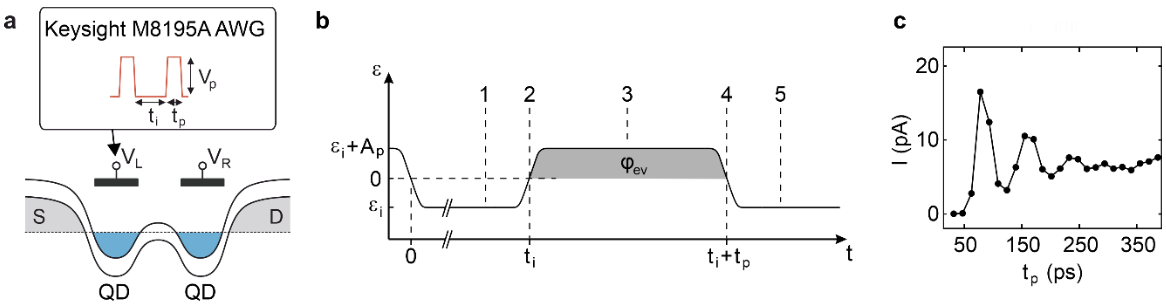

Figure 3. a A Keysight M8195A arbitrary waveform generator applies pulse sequences with a sampling rate of 65 GS/s to one of the gates. **b** Pulse sequence characterized by amplitude A_p and durations t_p and t_i applied to drive the system across the detuning. After initialization in the ground state $|R\rangle$, the system is detuned such that at $\varepsilon = 0$ a Landau-Zener transition into the excited state $|L\rangle$ is possible which creates a superposition state. Both components of the wave function evolve separately accumulating a relative phase φ_ev and interfere when crossing $\varepsilon = 0$ again. The readout can distinguish between the states $|L\rangle$ and $|R\rangle$. **c** Coherent charge oscillations in the time domain.

Configuration of control instruments

The graphene quantum device is controlled by RF and DC voltages applied to the gates of the device. Depending on the type of experiment, continuous wave microwave signals with frequencies up to 30 GHz are generated by a E8257D analog signal generator or pulse sequences with a sampling rate of 65 GS/s are generated by an AWG M8195A. The RF signals are attenuated inside the cryostat and combined with DC voltages through bias tees on a custom-made printed circuit board (PCB). Using a home-built IV-converter, the current through the device is amplified and converted into a voltage which is measured by a Keysight DMM 34410A. Figure 4 shows a typical configuration of the experimental setup.

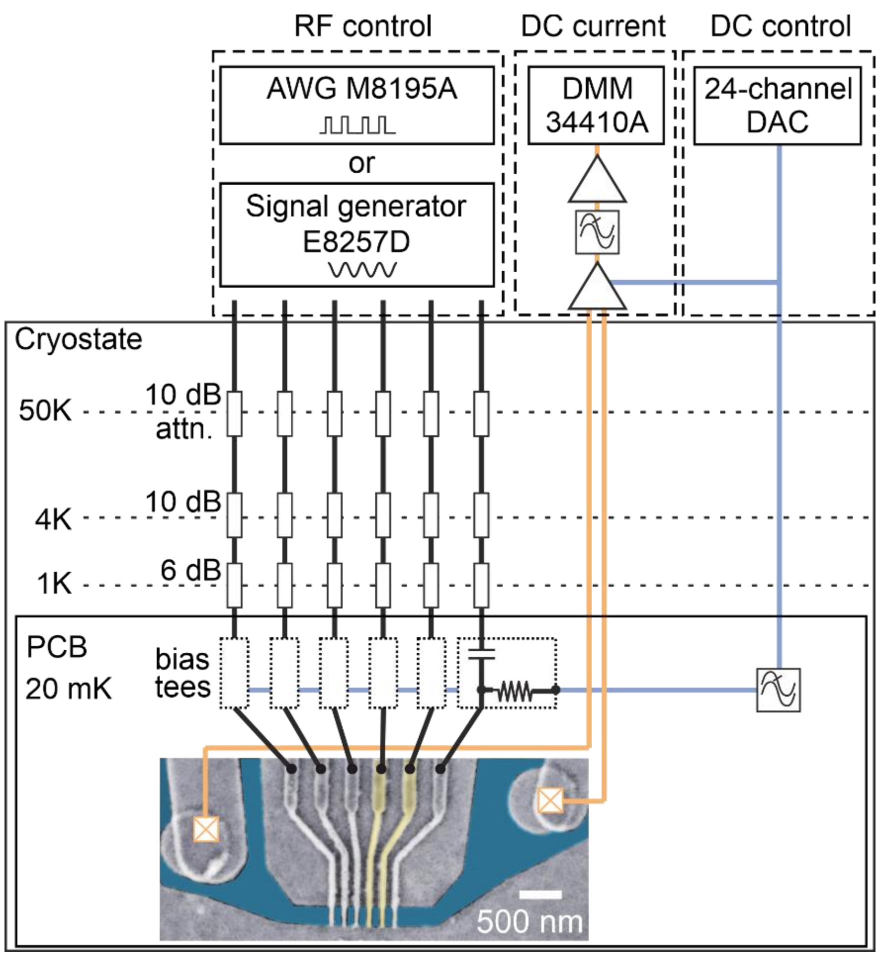

Figure 4. Schematic of the typical configuration of the measurement equipment and the cryostat used for coherence experiments on bilayer graphene quantum devices.

Measurement control using Labber

In this section, we show how the coherence experiments can be controlled via the software Labber. This lab-control software package consists of three modules: The Instrument Server handles the communication with the equipment. The Measurement Editor runs the experiment and handles the data acquisition. The Log Browser allows a fast plotting of the data and comes with basic analysis tools. In the following, we will illustrate the use of Labber as the control software for a charge coherence experiment.

Instrument Server

The Instrument Server (see Figure 5) acts as the link between the Measurement Editor which controls the actual experiment and the physical instruments. It handles the drivers and establishes the communication with all measurement hardware. Instruments can be added to the server from a database of predefined drivers which cover many DC and RF instruments. Furthermore, users can write customized drivers.

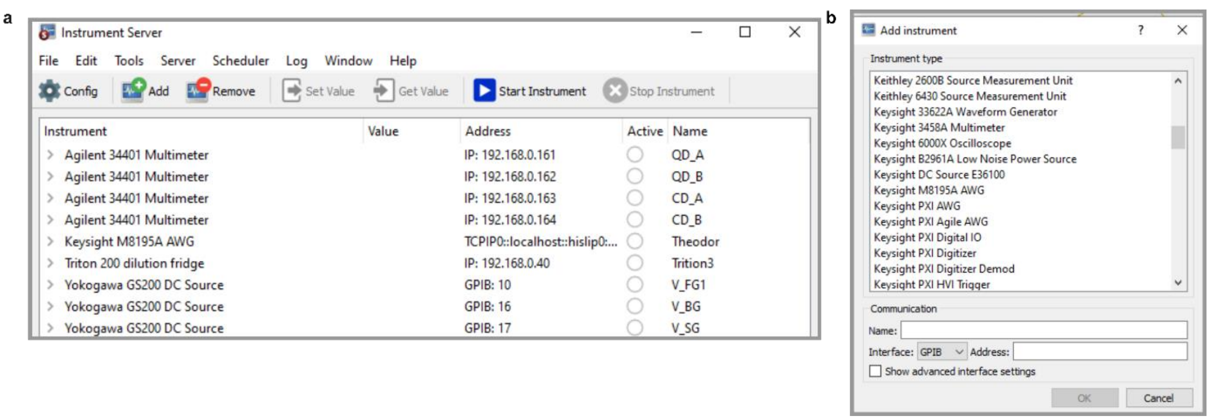

Figure 5. a Screenshot of Instrument server listing the connected instruments. **b** Instruments such as the Keysight M8195A AWG can be added from a database.

Pulse control

Beside physical instruments, the Instrument Server handles virtual instruments which address routines for a specific purpose without direct communication to the measurement hardware. Examples can be waveform generation or on-the-fly analysis. Here, the virtual driver 'Multi-qubit pulse generator' dedicated for qubit experiments is used to generate pulse trains with variable width and amplitude. The virtual driver hands over the waveform to the instrument driver. Figure 6 shows an example of such a sequence.

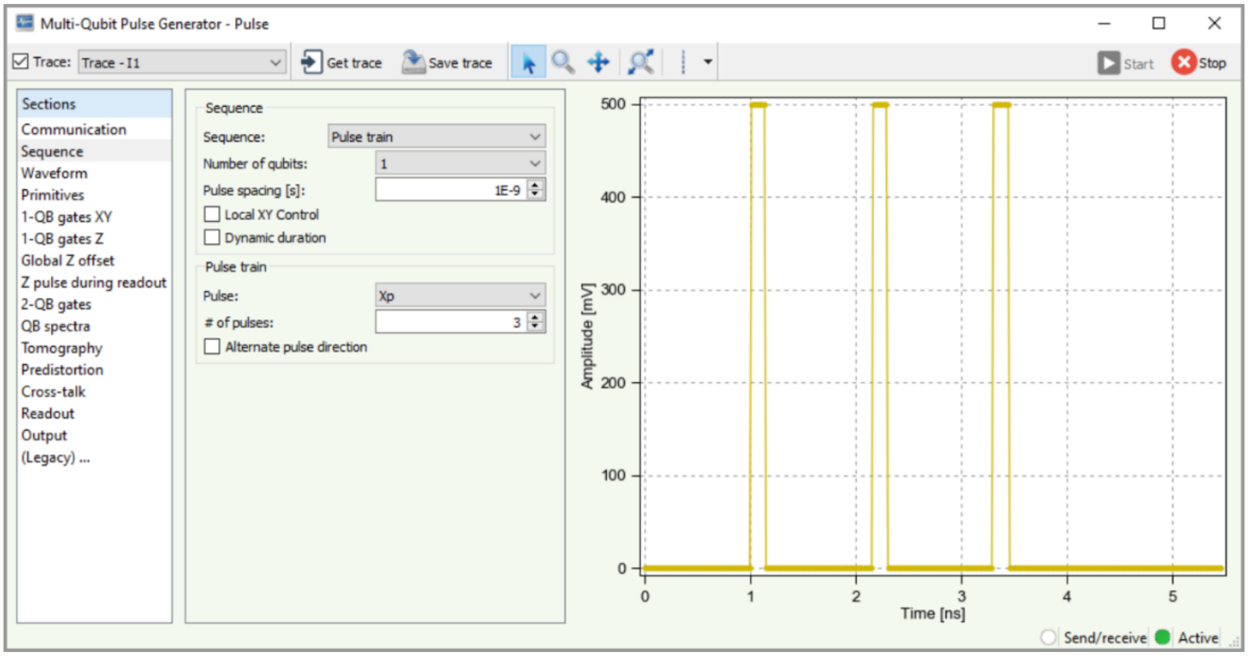

Figure 6. Screenshot of a virtual driver 'Multi-qubit pulse generator' displaying a preview of the pulse train.

Measurement Editor

In the Measurement Editor the experiment is composed. The required instruments are added from the server. Via 'Signal Connections' virtual instruments are linked to output channels of physical instruments. In 'Step sequence' a set of measurement instructions is defined while in 'Log Channels' the measured parameters are specified. 'Start Measurement' runs the measurement and stores the acquired data together with all instrument settings in the meta data in the. hdf5 file format.

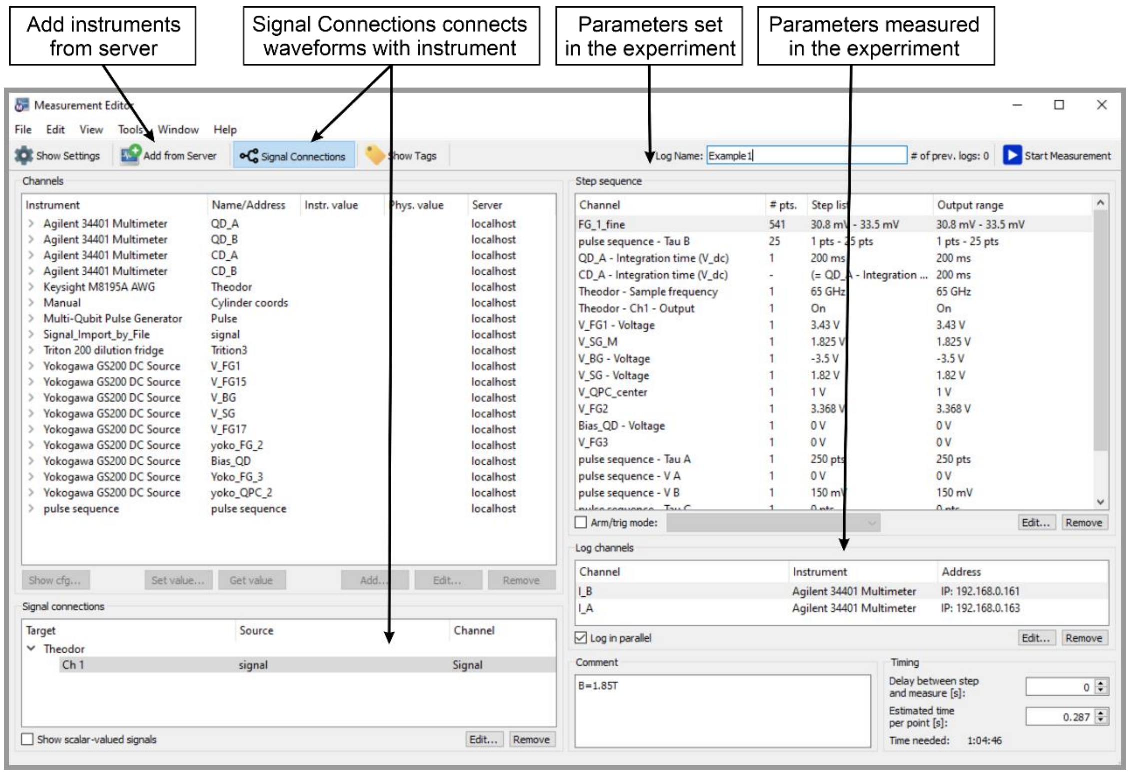

Figure 7. Example showing the Measurement Editor where pulse sequence will be output on an AWG channel.

Log Browser

All measurements performed via the Measurement Editor is stored in individual hdf5 files. Those can be opened in any desired environment. The Log Browser offers a convenient way to browse through measurements data avoiding the need to import data in an external analysis tool. It shows a preview of data sets and displays the measurement configuration. Data sets can be filtered e.g. by date, username or keyword.

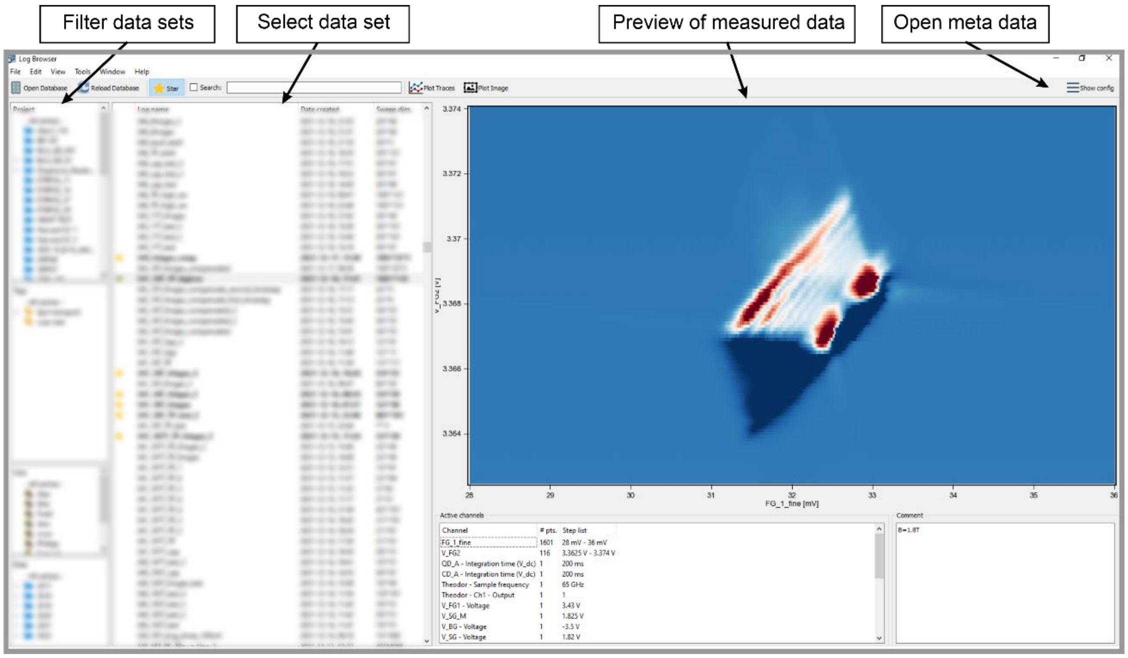

Figure 8. Log Browser showing a list of measurements and the preview of a specific data set.

Furthermore, the Log Browser can open data sets in a viewer mode, which offers basic data analysis functionality. Data export to other file formats and image formats is possible.

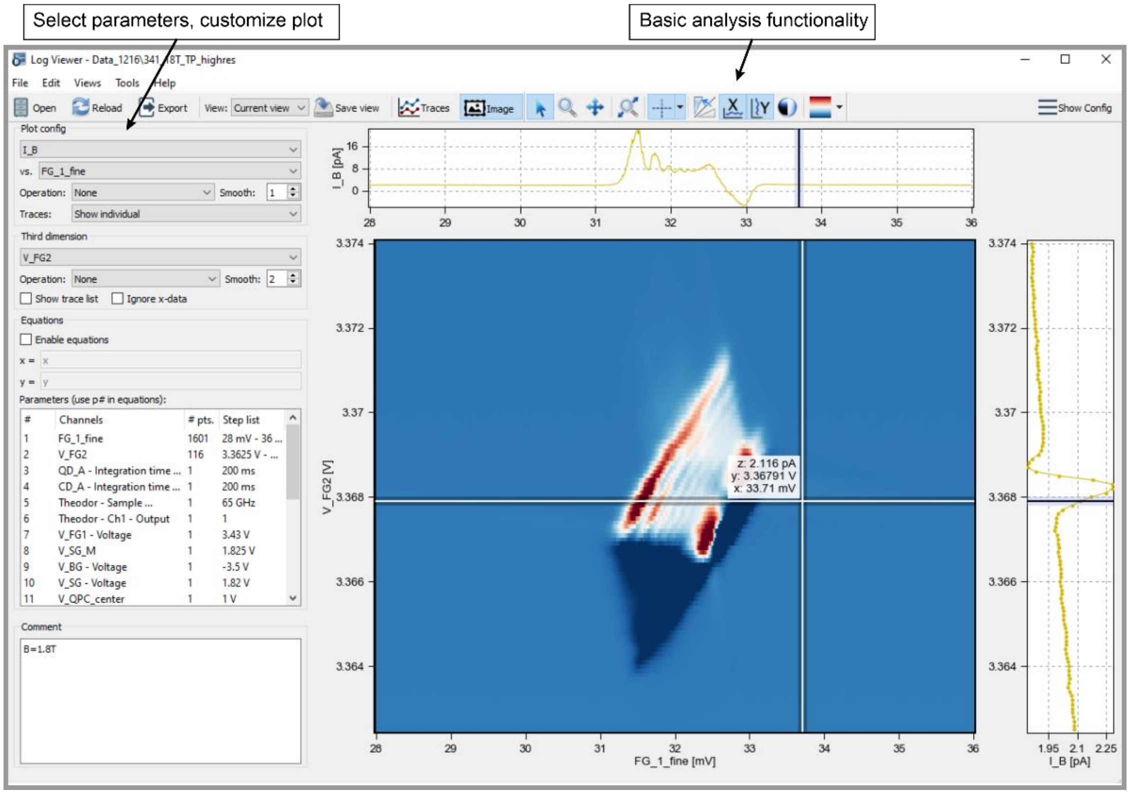

Figure 9. Log Viewer showing a data set together with line cuts along x and y direction.

Conclusion

In this application note, we have discussed the use-case of charge coherence experiments in bilayer graphene quantum dots. These experiments require fast operation times with pulse durations down to tens of picoseconds. This high demand is met by the AWG M8195A offering a sampling rate of 65 GS/s. All experiments have been conducted with Labber. The intuitive user interface allows a convenient of defining pulse sequences. The virtual driver 'Multi-qubit pulse generator' brings the functionality for future qubit experiments.

KEYSIGHT

Keysight enables innovators to push the boundaries of engineering by quickly solving design, emulation, and test challenges to create the best product experiences. Start your innovation journey at www.keysight.com.